

20. M. D. Marmor, Y. Yarden, *Oncogene* **23**, 2057 (2004).
 21. Y. Katoh et al., *J. Biol. Chem.* **279**, 24435 (2004).
 22. C. B. Thien, W. Y. Langdon, *Nat. Rev. Mol. Cell Biol.* **2**, 294 (2001).
 23. K. Haglund et al., *Nat. Cell Biol.* **5**, 461 (2003).
 24. F. Debais et al., *Exp. Cell Res.* **297**, 235 (2004).
 25. R. Fukuyama et al., *Biochem. Biophys. Res. Commun.* **315**, 636 (2004).
 26. N. Ghosh-Choudhury et al., *J. Biol. Chem.* **277**, 33361 (2002).
 27. F. Vinals, T. Lopez-Rovira, J. L. Rosa, F. Ventura, *FEBS Lett.* **510**, 99 (2002).
 28. M. F. Favata et al., *J. Biol. Chem.* **273**, 18623 (1998).
 29. C. F. Lai et al., *J. Biol. Chem.* **276**, 14443 (2001).
 30. T. Okada, L. Sakuma, Y. Fukui, O. Hazeki, M. Ui, *J. Biol. Chem.* **269**, 3563 (1994).
 31. T. F. Franke et al., *Cell* **81**, 727 (1995).
 32. B. M. Abdallah et al., *Biochem. Biophys. Res. Commun.* **326**, 527 (2005).
 33. Materials and methods are available as supporting material on Science Online.
 34. We thank all members of our laboratory for help and fruitful discussions, especially C. de Hoog for critical reading of the manuscript, J. V. Olsen for help with the LTQ-FT and statistical analysis and S.-E. Ong for help with data analysis. We thank I. Dikic for the kind gift of hemagglutinin-tagged constructs of c-Cbl and Cbl-b. Work in CEBl is supported by a grant by the

Danish National Research foundation. This work was also supported by "Interaction Proteome," a 6th Framework program of the European Commission.

Supporting Online Material

www.sciencemag.org/cgi/content/full/308/5727/1472/DC1

Materials and Methods

Figs. S1 to S5

Table S1

References

17 November 2004; accepted 7 April 2005

10.1126/science.1107627

The Structure of Interleukin-2 Complexed with Its Alpha Receptor

Mathias Rickert,* Xinquan Wang,* Martin J. Boulanger, Natalia Goriatcheva, K. Christopher Garcia†

Interleukin-2 (IL-2) is an immunoregulatory cytokine that binds sequentially to the alpha (IL-2R α), beta (IL-2R β), and common gamma chain (γ_c) receptor subunits. Here we present the 2.8 angstrom crystal structure of a complex between human IL-2 and IL-2R α , which interact in a docking mode distinct from that of other cytokine receptor complexes. IL-2R α is composed of strand-swapped "sushi-like" domains, unlike the classical cytokine receptor fold. As a result of this domain swap, IL-2R α uses a composite surface to dock into a groove on IL-2 that also serves as a binding site for antagonist drugs. With this complex, we now have representative structures for each class of hematopoietic cytokine receptor-docking modules.

Interleukin-2 (IL-2), which is one of the first cytokines identified and a member of the four-helix bundle cytokine superfamily, acts at the heart of the immune response (1). IL-2 and its alpha receptor, IL-2R α , are expressed by T cells after the activation of T cell receptors by peptide-major histocompatibility complexes. The subsequent autocrine interaction of IL-2 with its receptors leads to the stimulation of signal transduction pathways resulting in T cell, B cell, and natural killer (NK) cell proliferation and clonal expansion (2).

The pleiotropic biological activities of IL-2 are mediated by three cell surface receptors: the IL-2R α chain; the IL-2R β chain; and the common gamma chain (γ_c), which is also a receptor for IL-4, IL-7, IL-9, IL-15, and IL-21 (3). These cell surface receptors form a complex that signals through the intracellular activation of the Janus tyrosine kinase 3 (Jak3) and the signal transducer and activator of transcription 5 (STAT5) (4). The IL-2R α chain, originally identified as the Tac antigen (CD25) (5–7), is enigmatic in that it lacks

signature features of the cytokine receptor superfamily (8). IL-2R β (p75) and the γ_c are both members of the hematopoietic growth factor receptor family, containing the signature cytokine-binding homology region (CHR), which is composed of two fibronectin type-III (FN-III) repeats (2, 8).

Biochemical studies show that the assembly of the IL-2 receptor complex is initiated by the interaction of IL-2 with IL-2R α , followed by sequential recruitment of IL-2R β and γ_c (9, 10). IL-2R α alone is the "low-affinity" receptor (dissociation constant $K_d \sim 10$ nM). When expressed together, IL-2R α and IL-2R β form the pseudo-high-affinity receptor ($K_d \sim 30$ pM). Finally, the IL-2R $\alpha\beta\gamma_c$ complex forms the high-affinity receptor ($K_d \sim 10$ pM) that is the signaling complex found on activated T cells (2). The IL-2R β and γ_c binding sites on IL-2 have been mapped to locations analogous to the site I and site II cytokine-binding sites originally established in the human growth hormone (hGH) system (11). However, based on sequence analysis and mutagenesis studies, IL-2R α is predicted to differ from other cytokine receptors in both its structure and its mode of interaction with IL-2 (12).

IL-2R α is a target for therapeutic modulation because it is not expressed on resting T and B cells but is continuously expressed by the abnormal T cells of patients with forms of

leukemia, autoimmunity, and organ transplant rejection (13, 14). An antagonistic monoclonal antibody to IL-2R α (anti-Tac) (Daclizumab) is effective in preventing the rejection of organ transplants (15). Small-molecule inhibitors of IL-2R α have also been developed (16, 17). IL-2 (Proleukin) itself is used to augment immune system function and has efficacy in treating metastatic renal carcinoma and melanoma (18). However, there is severe dose-limiting toxicity that is largely attributed to activation of the $\beta\gamma_c$ form of the receptor on NK cells (18). Currently, no structural information exists for any of the IL-2 receptors, and this information could assist in the design of improved therapeutics. Here we present a crystal structure at 2.8 Å resolution of human IL-2 in complex with the extracellular domain of IL-2R α (19).

In the complex structure, the IL-2R α ectodomain resembles an arm bent $\sim 90^\circ$ at the elbow between the N- and C-terminal domains (D1 and D2, respectively), engaging IL-2 along the length of the underside of D1 (Fig. 1, A and B). The IL-2 binding surface comprises helix A', helix B', and part of the AB loop. The long axes of the IL-2R α β sheets are aligned parallel with the helical axes of the cytokine. This differs from the typical cytokine receptor interaction. For example, in the complex of hGH with its receptor (hGH-R), the CHR module of hGH-R, composed of two β -sandwich FN-III domains, forms a considerably larger, but similar, bent arm-like structure (Fig. 1B) (20). However, the protruding elbow region of hGH-R exposes loops that bind to the sides of the hGH four-helix bundle (20) (Fig. 1B). Although substantially different, the closest similarity can be found in the recently elucidated site III contact between gp130-class cytokines and the gp130 D1 domain (21). However, in that interaction, the cytokine forms contacts exclusively through loops at the tip of the cytokine, rather than with residues on the helical surfaces.

In the IL-2R α structure, the core D1 and D2 domains are separated by a 42-residue interdomain linker peptide (Thr⁶⁵ to His¹⁰³), and the second domain has an additional C-terminal 54-residue connecting peptide leading to the cell membrane (Gly¹⁶⁵ to Glu²¹⁷). Neither of these linkers is visible in the electron density

Departments of Microbiology and Immunology, and Structural Biology, Stanford University School of Medicine, 299 Campus Drive, Fairchild D319, Stanford, CA 94305-5124, USA.

*These authors contributed equally to this work.

†To whom correspondence should be addressed. E-mail: kcgarcia@stanford.edu

map, and they are therefore not included in the IL-2R α model (Fig. 1A). These linker segments do not contribute to ligand binding. Thus, 120 residues (D1 and D2 domains) of the 217-amino acid extracellular domain are structured. It is possible that this extensive amount of flexible polypeptide contributed to the difficulties in obtaining crystals suitable for a structure determination, as crystallization of the complex was originally reported in 1989 (22).

IL-2R α deviates from the classical cytokine receptor fold, both in the structures of the individual domains and in the interdomain folding topology (Fig. 1A). Each of the two IL-2R α domains exhibits ~30% amino acid homology to a group of β -sandwich protein domains variously called sushi domains, short consensus repeats (SCRs), or complement control protein (CCP) repeats (23) (Fig. 2B). Canonical sushi domains (~65 amino acids in a 2-on-3 sandwich) can be considered “mini” FN-III-type domains (~110 residues in a 3-on-4 sandwich). Like sushi domains, IL-2R α

D1 (residues 1 to 64) and D2 (residues 104 to 165) show an elliptical β -sandwich structure, containing several residues that are highly conserved in sushi domains of several complementary related proteins (Cys^{3/30/46/61}, Pro⁷, Tyr²⁰, Gly³³, Phe³⁴, and Trp⁵⁵) (24). However, both IL-2R α domains deviate substantially from canonical sushi topology; they are 1-on-4, instead of 2-on-3, β sandwiches. The folding topology of IL-2R α also exhibits swapping of β strands across the N- and C-terminal sushi-like domains (Fig. 2A). Strands A and B exchange with strands F and G, respectively, to give the folding topology F-on-G-C-D-E for D1 and A-on-B-H-I-J for D2. Interdomain disulfide bonds between Cys³ and Cys⁴⁶ of D1 and Cys¹⁴⁷ and Cys¹⁰⁴ of D2 enforce the strand exchange by pinning strand A of D1 to strand I of D2 and strand G of D2 to strand D in D1 (Figs. 1A and 2A). This strand exchange has not been seen among β -sandwich-type structures (Fig. 2B), or in classical FN-III-type cytokine receptors. The IL-15 α recep-

tor is a single sushi domain, so there is not the possibility for a strand exchange in that case.

Despite the unstructured 42-amino acid linker peptide in IL-2R α , the D1 and D2 domains are in intimate contact with one another through an extensive interdomain interface. A large hydrophobic core is formed between the swapped top strands in each domain, which likely imparts rigidity to the overall structure (Fig. 1A). These exposed aromatics on the surface of the top strands of the β sandwich would serve as the inner hydrophobic core between the top and bottom sheets of a canonical sushi domain, if the strands in IL-2R α were not domain-swapped.

The IL-2 molecule has the common cytokine fold (8), with the typical up-up-down-down four-helix topology. The four-helix bundle structure of the IL-2 molecule in the IL-2/IL-2R α complex closely superimposes with the free IL-2 molecule [0.74 Å root mean square deviation (RMSD) on 76 C α positions], but with minor structural adapta-

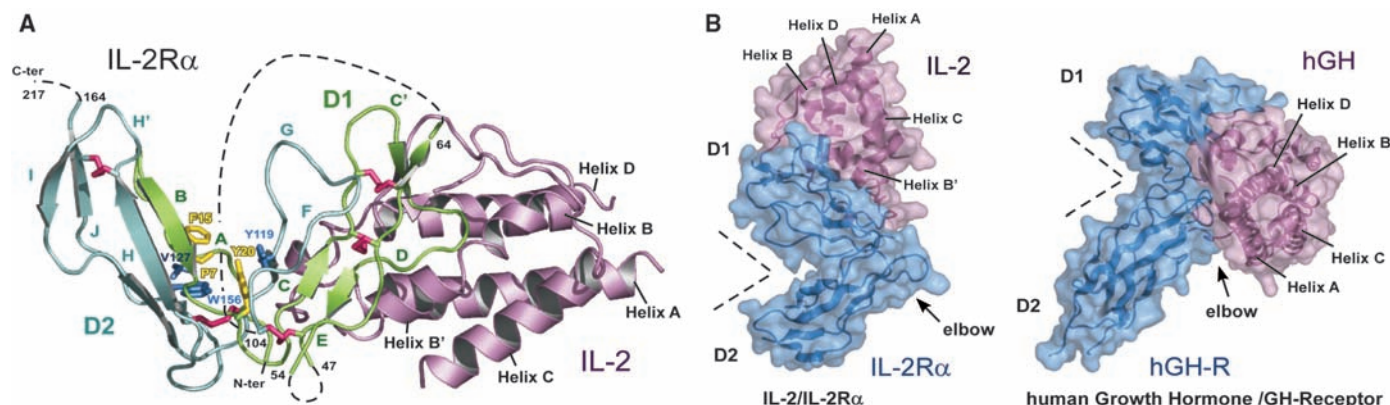
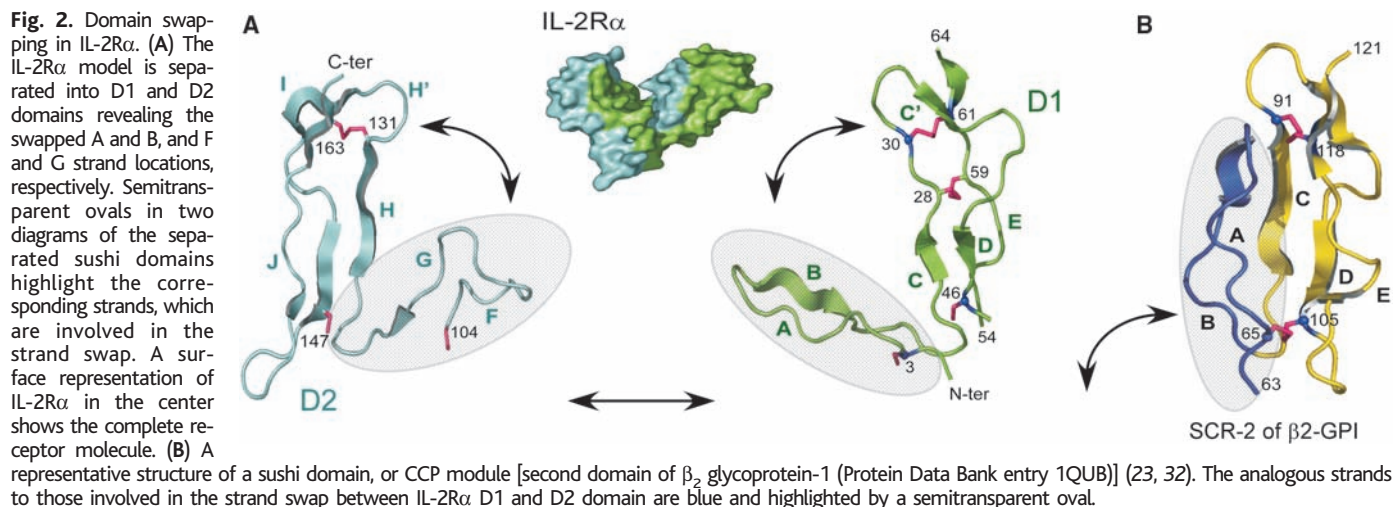


Fig. 1. Structure of the human IL-2/IL-2R α complex. (A) Side view of the complex showing IL-2R α covering the groove between the AB loop and helix B'. The IL-2R α D1 domain is green, the D2 domain is cyan, and IL-2 is violet. Disulfide bonds of IL-2R α are pink. Hydrophobic core residues between D1 and D2 are drawn as yellow and blue sticks, respectively. Disordered connecting regions, which are not part of the experimental model, are

shown as black dotted lines. This coloring scheme is maintained in Figs. 1 to 4. (B) The binding mode between IL-2 and IL-2R α versus the classical site I/II paradigm of hGH and its receptor, in which the elbow of the receptor binds to the sides of the cytokine four-helix bundle (20). A semitransparent surface representation with receptor chains in blue and ligands in violet is shown. Black dotted vees indicate the elbow regions of IL-2R α and hGH-R.



tions in the receptor binding site (25, 26). The IL-2 CD loop, which is usually disordered in uncomplexed IL-2 structures, is completely ordered in the receptor-bound IL-2 structure because residues Glu¹⁰⁶ to Asp¹⁰⁹ are involved in binding to IL-2R α . The first and last turn of helix A' as well as the last turn of helix B' are partially unwound as compared with free IL-2 (fig. S1).

The interaction between IL-2 and IL-2R α occurs between the four-stranded β sheet, strands G-C-D-E, and the IL-2 A' and B' helices (Fig. 3A). As a result of complex formation, 20 IL-2 residues and 21 IL-2R α residues bury a total of 1868 Å² (fig. S2 and table S2). Two prominent hydrophobic patches on IL-2 are consistent with thermodynamic

measurements indicating that the desolvation of apolar surface is the primary energetic driving force of this interaction (red amino acids in Fig. 3B and red patches in Fig. 4A). The first patch is composed of Tyr⁴⁵ on the AB loop of IL-2, which packs into a pocket formed by the methylene groups of Arg³⁵ and Arg³⁶ of the IL-2R α C' strand. This hydrophobic cluster is surrounded by polar interactions. Mutations of IL-2R α Arg³⁵ and Arg³⁶ disrupt interaction with IL-2 (27).

The most conspicuous and centrally located hydrophobic cluster is composed of Phe⁴² and Leu⁷² on the IL-2 AB loop and helix B', respectively, inserting into a recessed pocket on IL-2R α composed of Leu⁴² to Tyr⁴³, and Met²⁵ (fig. S4 and Figs. 3B and

4A). Several salt bridges and hydrogen bonds surround this hydrophobic patch (Fig. 3A and table S2). Mutational studies identify this second hydrophobic region around IL-2 Phe⁴² as the primary energetic determinant in the IL-2-binding epitope (27, 28). T cells can express IL-2 splice variants, which are natural inhibitors of IL-2 signaling through the high-affinity $\alpha\beta\gamma_c$ receptor (29). The splice variants lack either exon 2 (IL-2 δ 2), which encodes Asn³⁰ to Lys⁴⁹, or exon 3 (IL-2 δ 3), which encodes Ala⁵⁰ to Lys⁹⁷. Because these regions are involved in the interaction between IL-2R α and full-length IL-2, the splice variants would almost certainly not bind IL-2R α . Thus, the mechanism of inhibition appears to be the occupation of the IL-2R β and γ_c receptors, preventing recruitment of IL-2R α by wild-type IL-2 and inhibiting signaling on activated T cells through the $\alpha\beta\gamma_c$ complex.

The disruption of protein-protein interactions with small molecules has proven to be an exceedingly difficult goal for the pharmaceutical industry in comparison to the inhibition of enzyme active sites. However, potent small-molecule inhibitors of the IL-2/IL-2R α interaction have been developed (17). One of these small molecules, compound 1 (16), fits into a groove between the IL-2 AB loop and helix B', wrapping around IL-2 Phe⁴² as a hydrophobic anchor residue (Fig. 4B) (17). In binding to IL-2, the small molecule induces the rearrangement of residues Lys³⁵, Arg³⁸, Met³⁹, and Phe⁴², compared with several unliganded IL-2 structures (17). In particular, a large change in conformation of the IL-2 Phe⁴² aromatic ring creates the recessed channel used for binding the drug (Fig. 4B). This conformational adjustment does not occur upon receptor binding; in contrast, Phe⁴² is a prominent knob fitting into a pocket on IL-2R α . Superposition of the drug/IL-2 complex on the IL-2/

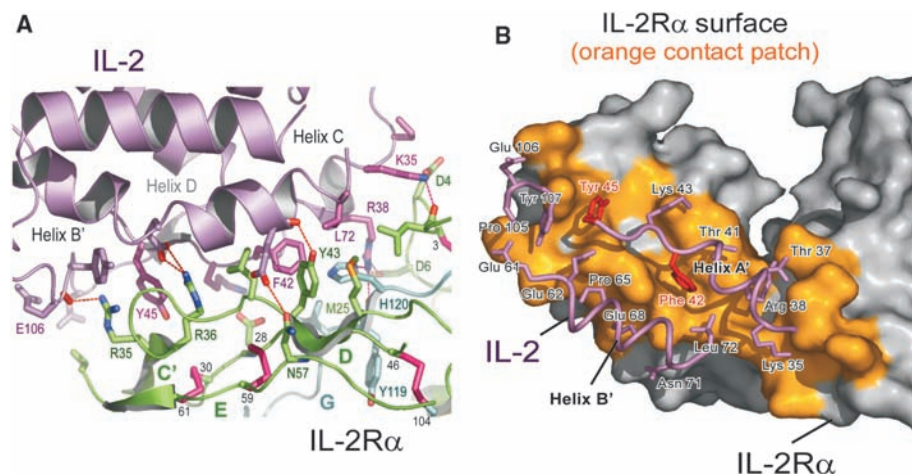
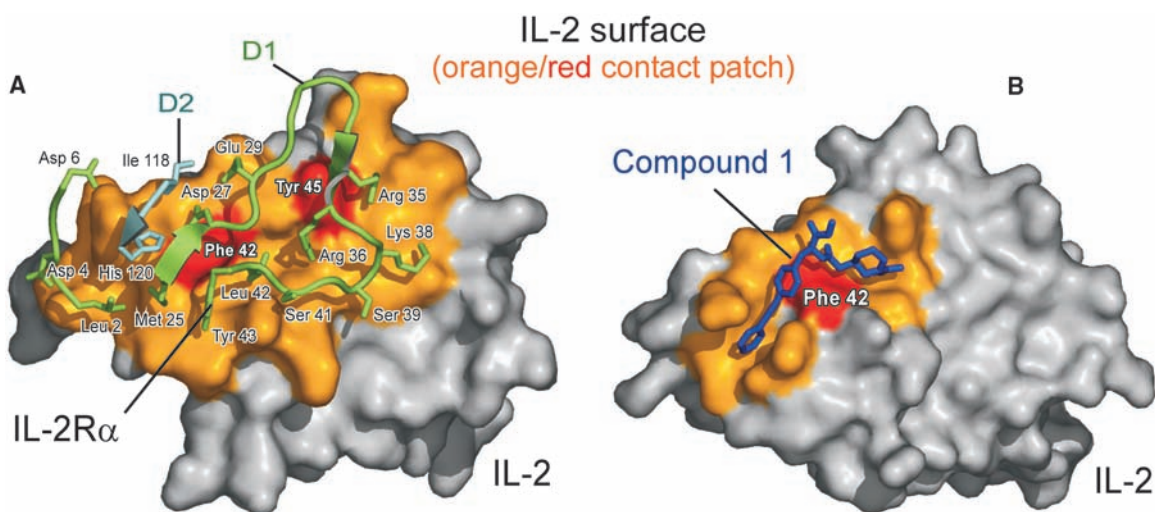


Fig. 3. Molecular anatomy of the IL-2/IL-2R α interface. (A) Amino acid contact residues within the complex interface. IL-2 (violet) is at the top and the IL-2R α D1 domain (green) and D2 domain (cyan) are at the bottom. Hydrogen bonds appear as red dotted lines; disulfide bonds are pink; corresponding cysteine residues are numbered; and β sheets and connecting loops of IL-2R α are labeled as indicated. (B) "Footprint" surface representation of the IL-2R α interface viewed through the IL-2 helices onto the IL-2R α . Contact residues of IL-2 (violet sticks) are projected onto the buried surface (orange) of IL-2R α . The hydrophobic anchor residues Phe⁴² and Tyr⁴⁵ of IL-2 are colored red to orient the reader throughout the interface.

Fig. 4. Comparison of receptor versus drug binding to IL-2. (A) "Footprint" representation of IL-2 interface as viewed through the IL-2R α β strands onto the IL-2 surface. Contact residues of IL-2R α (green and cyan sticks) are projected onto the buried surface (orange) of IL-2. The hydrophobic anchor residues Phe⁴² and Tyr⁴⁵ of IL-2 are red. (B) Analogous footprint view of the drug compound 1 bound to IL-2. Compound 1 is depicted with blue sticks [Protein Data Bank entry name 1M48 (17)] projected onto the buried surface (orange) of IL-2. Compound 1 uses IL-2 Phe⁴² (red patch) as an anchor residue, thereby preventing IL-2R α from binding to IL-2.



IL-2R α complex reveals that although a substantial portion of the drug fits within open space in the interface, there are steric clashes with the IL-2 Phe⁴² binding pocket. The drug apparently uses highly favorable enthalpic interactions to compensate for the entropic penalty of binding (17) and to overcome its small buried surface area. In contrast, binding of IL-2R α to IL-2 is entropically favorable. Hence, even though the drug and receptor target a similar hydrophobic hot spot, they use opposite thermodynamic solutions for binding.

Previously determined binding modes between hematopoietic cytokines and their receptors involve combinations of the classical site I/II and the recently determined site III mode for gp130 cytokines (21). We suggest that the distinctive docking geometry of the IL-2/IL-2R α interaction is a fourth binding mode and now gives us representative examples of all binary recognition modules used by hematopoietic receptors to recognize four-helix cytokines. These four modules can be used as building blocks, in different combinations, to construct topological models for complexes between all known cytokines and their receptors. As discussed, IL-2 also binds to two additional receptor subunits, the IL-2R β and γ_c chains, to form a quaternary signaling complex. Functional studies and molecular modeling placed the binding epitopes of IL-2R β and γ_c on the faces of adjacent helices A (IL-2 Asp²⁰) and D (IL-2 Gln¹²⁶),

respectively (11, 14, 30) (figs. S1 and S5). It has been postulated that IL-2R β will bind in site I-type and γ_c will bind in site II-type geometries (Fig. 1B, hGH complex). The binding site of IL-2R α is ideal for an initial engagement of cytokine, leaving sides of the helical faces open for engagement of the IL-2R β and γ_c components. By initially capturing IL-2 on the cell surface, the IL-2R α would reduce the entropic cost for the subsequent recruitment of additional receptors (31).

References and Notes

1. K. A. Smith, *Science* **240**, 1169 (1988).
2. B. H. Nelson, D. M. Willerford, *Adv. Immunol.* **70**, 1 (1998).
3. P. E. Kovanen, W. J. Leonard, *Immunol. Rev.* **202**, 67 (2004).
4. Y. Minami, T. Kono, T. Miyazaki, T. Taniguchi, *Annu. Rev. Immunol.* **11**, 245 (1993).
5. T. Uchiyama et al., *J. Clin. Invest.* **76**, 446 (1985).
6. W. J. Leonard et al., *Nature* **300**, 267 (1982).
7. W. J. Leonard et al., *Nature* **311**, 626 (1984).
8. J. F. Bazan, *Proc. Natl. Acad. Sci. U.S.A.* **87**, 6934 (1990).
9. S. F. Liparoto, T. L. Ciardelli, *J. Mol. Recognit.* **12**, 316 (1999).
10. M. Rickert, M. J. Boulanger, N. Goriatcheva, K. C. Garcia, *J. Mol. Biol.* **339**, 1115 (2004).
11. P. Bamborough, C. J. Hedgecock, W. G. Richards, *Structure* **2**, 839 (1994).
12. R. M. Stroud, J. A. Wells, *Sci. STKE* **2004**, re7 (2004).
13. A. C. Church, *Q. J. Med.* **96**, 91 (2003).
14. J. Theze, P. M. Alzari, J. Bertoglio, *Immunol. Today* **17**, 481 (1996).
15. T. A. Waldmann, J. O'Shea, *Curr. Opin. Immunol.* **10**, 507 (1998).
16. J. W. Tilley et al., *J. Am. Chem. Soc.* **119**, 7589 (1997).
17. M. R. Arkin et al., *Proc. Natl. Acad. Sci. U.S.A.* **100**, 1603 (2003).

18. J. W. Eklund, T. M. Kuzel, *Curr. Opin. Oncol.* **16**, 542 (2004).
19. Materials and methods are available as supporting material on Science Online.
20. A. M. de Vos, M. Ultsch, A. A. Kossiakoff, *Science* **255**, 306 (1992).
21. M. J. Boulanger, D. C. Chow, E. E. Brevnova, K. C. Garcia, *Science* **300**, 2101 (2003).
22. G. Lambert, E. A. Stura, I. A. Wilson, *J. Biol. Chem.* **264**, 12730 (1989).
23. M. Baron, D. G. Norman, I. D. Campbell, *Trends Biochem. Sci.* **16**, 13 (1991).
24. D. A. Shackelford, I. S. Trowbridge, *EMBO J.* **5**, 3275 (1986).
25. B. J. Brandhuber, T. Boone, W. C. Kenney, D. B. McKay, *Science* **238**, 1707 (1987).
26. J. F. Bazan, *Science* **257**, 410 (1992).
27. R. J. Robb, C. M. Rusk, M. P. Neeper, *Proc. Natl. Acad. Sci. U.S.A.* **85**, 5654 (1988).
28. K. Sauve et al., *Proc. Natl. Acad. Sci. U.S.A.* **88**, 4636 (1991).
29. V. N. Tsytsikov, V. V. Yurovsky, S. P. Atamas, W. J. Alms, B. White, *J. Biol. Chem.* **271**, 23055 (1996).
30. S. M. Zurawski, J. L. Imler, G. Zurawski, *EMBO J.* **9**, 3899 (1990).
31. Z. Wu et al., *J. Biol. Chem.* **270**, 16039 (1995).
32. R. Schwarzenbacher et al., *EMBO J.* **18**, 6228 (1999).
33. We thank K. A. Smith, J. F. Bazan, P. Strop, D. McKay, B. Weis, and D. Bushnell for helpful discussions. This work was funded by grants from the Keck Foundation, Pew Trust, and NIH (AI51321). The coordinates and structural factors have been deposited in the Protein Data Bank with accession no. 1Z92.

Supporting Online Material

www.sciencemag.org/cgi/content/full/308/5727/1477/DC1

Materials and Methods
Figs. S1 to S5
Tables S1 and S2
References

13 January 2005; accepted 7 April 2005
10.1126/science.1109745

A Fluoroquinolone Resistance Protein from *Mycobacterium tuberculosis* That Mimics DNA

Subray S. Hegde,^{1*} Matthew W. Vetting,^{1*} Steven L. Roderick,¹ Lesley A. Mitchenall,² Anthony Maxwell,² Howard E. Takiff,³ John S. Blanchard^{1†}

Fluoroquinolones are gaining increasing importance in the treatment of tuberculosis. The expression of MfpA, a member of the pentapeptide repeat family of proteins from *Mycobacterium tuberculosis*, causes resistance to ciprofloxacin and sparflaxacin. This protein binds to DNA gyrase and inhibits its activity. Its three-dimensional structure reveals a fold, which we have named the right-handed quadrilateral β helix, that exhibits size, shape, and electrostatic similarity to B-form DNA. This represents a form of DNA mimicry and explains both its inhibitory effect on DNA gyrase and fluoroquinolone resistance resulting from the protein's expression in vivo.

Increasing resistance to two bactericidal compounds that act on rapidly growing *Mycobacterium tuberculosis*, isoniazid and rifampicin, is driving the search for new therapies. Fluoroquinolones exert their powerful antibacterial activity by interacting with DNA gyrase and DNA topoisomerase IV (1). They bind reversibly to the enzyme-DNA complex

and stabilize the covalent enzyme tyrosyl-DNA phosphate ester, which is normally a transient intermediate in the topoisomerase reaction. Hydrolysis of this linkage leads to the accumulation of double-stranded DNA fragments and is the bactericidal consequence of fluoroquinolone treatment. Newer fluoroquinolones, including moxifloxacin and gatifloxacin,

exhibit powerful in vitro activity against mycobacteria (2, 3), and they can reduce multidrug treatment regimens from 6 to 4 months when substituted for isoniazid (4). Resistance to fluoroquinolones remains rare in clinical isolates of *M. tuberculosis* (5), but it has been increasing as their use in the treatment of multidrug-resistant *M. tuberculosis* infections increases (6). High-level resistance to fluoroquinolones in laboratory strains of *M. tuberculosis* and *M. smegmatis* (7, 8) is known to result from amino acid substitutions in the putative fluoroquinolone binding region of the *M. tuberculosis gyrA*-encoded A subunit of DNA gyrase (7, 8). This is the only type II topoisomerase encoded in the *M. tuberculosis* genome (9) and thus is the unique target for fluoroquinolones in this organism (10, 11).

¹Department of Biochemistry, Albert Einstein College of Medicine, 1300 Morris Park Avenue, Bronx, NY 10461, USA. ²Department of Biological Chemistry, John Innes Centre, Colney Lane, Norwich NR4 7UH, UK. ³Laboratorio de Genética Molecular, Centro de Microbiología y Biología Celular, Instituto Venezolano de Investigaciones Científicas, Caracas 1020A, Venezuela.

*These authors contributed equally to this work.
†To whom correspondence should be addressed.
E-mail: blanchar@aecom.yu.edu